

Published in final edited form as:
*Nano Lett*. 2011 February 9; 11(2): 512–517. doi:10.1021/nl103369g.

# The Fabrication of Sub-5-nm Nanochannels in Insulating Substrates using Focused Ion Beam Milling

**Laurent D. Menard** and **J. Michael Ramsey***
Department of Chemistry, University of North Carolina at Chapel Hill, Chapel Hill, NC 27599

## Abstract

The use of focused ion beam (FIB) milling to fabricate nanochannels with critical dimensions extending below 5 nm is described. FIB milled lines have narrowing widths as they are milled deeper into a substrate. This focusing characteristic is coupled with a two-layered architecture consisting of a relatively thick (>100 nm) metal film deposited onto a substrate. A channel is milled through the metal layer until it penetrates a prescribed depth into the substrate material. The metal is then removed, leaving a nanochannel with smooth surfaces and lateral dimensions as small as sub-5 nm. These open nanochannels can be sealed with a cover plate and the resulting devices are well-suited for single-molecule DNA transport studies. This methodology is used with quartz, single-crystal silicon, and polydimethylsiloxane substrates to demonstrate its general utility.

### Keywords

Nanochannels; nanofluidics; focused ion beam; FIB milling; DNA translocation

There has been considerable recent interest in the incorporation of nanoscale components in lab-on-a-chip fluidic devices. This interest owes its origin to several advantages (and differences that may be advantageously leveraged) in moving from the micron scale to the nanoscale. These differences include, for example, double-layer overlap (DLO) and its effect on electroosmosis and charge permselectivity, localized enhancement of electric fields, higher surface to volume ratios, confinement effects on large synthetic and bio-polymers, and the emerging importance of entropic effects.[1-3] The incorporation of nanoscale features in fluidic systems is by no means novel. Historic examples include the use of porous media and gels in chromatographic separations and the development of filtration membranes with nanoscale pores.[4,5] Recent efforts, however, have been focused on engineering geometrically well-defined conduits for fluid and analyte transport and seamlessly integrating them into devices.[6,7] The advantage of such regular structures is the relative simplicity of pressure and field gradients, fluid flow, and molecular motion contained within, in contrast to these properties in more tortuous networks. The capability to define, characterize, and easily model these systems enables better understandings of separation mechanisms and single molecule physics, for example.[6,8,9]

A number of fabrication tools have been brought to bear on the challenge of fabricating nanochannels. The methods suitable for nanochannel fabrication have been extensively reviewed.[10-13] Photolithography has been used to fabricate “nanoslits” - features with widths defined by the resolution limits of photolithography (i.e. usually several hundred nm to microns) and nanometer-scale depths defined by short duration wet or dry etching

*To whom correspondence should be addressed. jmramsey@unc.edu.

techniques.[14-16] Nanoimprint lithography has been shown capable of producing nanofluidic channels that are as small as 10 nm wide.[17] Electron beam lithography (EBL) has been used to pattern nanochannels etched into substrates using reactive ion etching (RIE) for use in DNA extension studies with dimensions as small as 50 nm.[18] Single DNA molecules have also been studied in focused ion beam (FIB) milled nanochannels on the order of 100 nm.[19,20] Various templating and molding strategies have also been used to generate nanochannels for nanofluidic studies in the 50-100 nm range.[21,22] Ultimate dimensions for templating strategies have extended below 10 nm, although channels this small have not been demonstrated as platforms in fluidic experiments.[23] Current efforts are underway to further develop these techniques to achieve structures with ever decreasing critical dimensions. In this vein, we describe a general methodology for the fabrication of nanochannels using FIB milling. The method involves milling channels in a substrate through a relatively thick (>100 nm) metal film. This metal layer serves several purposes. First, it allows the efficient conductance of charge in the case where the underlying substrate being patterned is electrically insulating. Second, and most importantly in these studies, it acts to partially mask the ion beam as the channel is milled progressively deeper. The milled feature's profile decreases as the depth increases due to several characteristics of the milling process: the Gaussian-like beam profile, the sputtering yield dependence on the angle of incidence (self-focusing), and the redeposition of material.[24,25] Third, it protects the substrate's top surface from redeposition of material and structural deformations typically observed along the edges of features milled directly into substrates.[26] Following the milling of channels into the substrate underlying the metal film, the metal is removed using a chemical etch and the nanoscale features are sealed with a cover plate to yield the final nanochannels. Given the direct-write nature of FIB milling, these nanochannels are easily interfaced to microchannels prepared using standard photolithography and wet etching methods. These steps are schematically illustrated in Figure 1. We have successfully prepared sealed nanochannels with an aspect ratio (depth:width) of ca. 1.0 for use in single molecule studies of DNA transport dynamics. Features with widths below 5 nm have been achieved.

This strategy has primarily been developed for the fabrication of nanochannels in quartz substrates as components in lab-on-a-chip devices. In this case, a chromium film was used as the conducting and masking layer. Chromium is well suited for this application given its low sputtering yield (0.10 $\mu m^3/nC$ for 30 keV $Ga^+$ ions at normal incidence) and ease of removal with chemical etchants.[27] Here we used a commercial Chromium Mask Etchant (Transene Company, Inc.). Quartz substrates with a 130-nm thick chromium film were used as received (Telic Co.) and thicker Cr films and Al films was deposited using ion beam sputtering (Model IBS/e, South Bay Technologies, Inc.). Nanochannels with relatively large critical dimensions (greater than ~30 nm in width) are milled by rastering the beam over a rectangular patterning region with a width approximately equal to the desired nanochannel width. The number of passes over the patterning region needed to achieve a nanochannel with the desired depth is dependent upon the ion beam current used and the metal film thickness. In fabricating a device, this depth setting is verified and optimized by milling test features, cross-sectioning and imaging them, and adjusting the depth setting to achieve the desired dimensions. Figure 2a-b,d-e shows 100-nm and 50-nm nanochannels milled into a quartz substrate through a 130-nm thick Cr film using an ion beam probe with a beam current of 50 pA and diameter (FWHM) of 20 nm. The nanochannels milled in this fashion have roughly square cross-sections with near vertical (7-10°) side walls. Operating in this mode, the width of the nanochannels obtained for a given film thickness and ion beam current is highly reproducible. It is controlled by the user-defined width of the scan area. The number of passes necessary to mill a desired depth into the substrate can vary slightly from sample to sample. It is sensitive to the thickness of the film, the ion beam focus conditions, and changes in the ion beam current. For samples with approximately identical

film thicknesses, these effects are generally small and only slight corrections are required from sample to sample.

Smaller nanochannels are milled by rastering the beam along a single line, with the channel width defined by the ion beam probe size and the metal film thickness. Using the smallest standard aperture (1.5 pA beam current, 7 nm probe diameter) available on a Helios NanoLab DualBeam Instrument (FEI Company) and milling through a 130-nm thick Cr film it has been possible to routinely mill channels with lateral dimension as small as 12-15 nm (Figure 2c,f). It is difficult to definitively characterize the cross-sectional shape of these channels but we estimate a roughly parabolic profile from the SEM images of the FIB-milled cross-sections. By simply increasing the Cr thickness to 300 nm it was possible to mill a channel that was less than 5-nm wide using the same ion beam conditions (Figure 3). When milling nanochannels using the smallest ion beam probes rastered along a line, the process is more sensitive to variations in the film thickness and ion beam focus conditions. Figure 4 shows the widths of nanochannels that were only just milled into quartz substrates through Cr films of various thicknesses, using an ion beam current of 1.5 pA. These data show a clear trend of decreasing channel size with increasing masking layer thickness. The data represent a series of different samples milled over several weeks on the instrument, indicating that channel widths obtained for a given film thickness are reproducible. We note that as the nanochannel dimensions decrease, the variance in their widths increases. In an effort to further decrease channel dimensions and improve uniformity, we are currently investigating the use of different masking layers and the effect of film smoothness. One caveat is that the total milling time increases with decreasing ion beam current and increasing metal film thickness. Consequently, under the conditions used to achieve nanochannels with critical dimensions in the 5-15 nm range, channel length is limited to approximately 10 microns, without stitching procedures. This is expected to be sufficiently long for many anticipated applications and longer milling times (and consequently longer channels) would be possible if compensation is made for sample drift.[28]

These FIB-milled nanochannels are only truly useful for nanofluidic experiments insofar as they can be sealed to form a fluidic network. This is achieved in quartz devices by fusion bonding of a quartz cover plate to the photolithographically and ion beam patterned substrate after the Cr film has been removed. The substrate and cover plate are cleaned using Nano-Strip™ 2X stabilized piranha solution (Cyantek Corporation), their surfaces are activated in an oxygen plasma (Harrick Plasma, 18 W, 10 min), and then they are brought into contact, forming a reversible bond. The bonding is made permanent by heating the device to 900°C in a furnace and holding at this temperature for >10 hrs. After bonding, the micro- and nanochannels are filled with an aqueous solution of fluorescent dye (2 mM fluorescein) and imaged using fluorescence microscopy to verify that the channels are open and continuous and the bonding is defect free. Figure 5a shows a fluorescence micrograph of nanochannels with a 30 nm × 30 nm cross-sectional area in such an experiment.

The quality of the nanochannel devices that are fabricated as described above are also evidenced by their utility in single molecule studies of DNA transport. In these experiments, fluorescently-stained double-stranded DNA molecules are electrophoretically driven through FIB-milled nanochannels of various sizes. Figure 5b shows individual frames from a recorded time series of the transport of a molecule of λ-phage DNA through a 50-μm long nanochannel with a 50 nm × 50 nm cross-sectional area. DNA molecules are transported smoothly through FIB-milled nanochannels as small as 15 nm × 15 nm with little evidence of adhesion. A constant electrophoretic mobility is observed over field strengths ranging from 200-25000 V $cm^{-1}$. Experiments can be run for several hours before the accumulation of DNA fragments (or solution impurities) on the nanochannel walls deleteriously affects device performance. These characteristics are indicative of nanochannels with extremely

low surface roughness, in contrast to nanochannels or nanoslits fabricated using RIE that can exhibit high surface roughness.[16,29,30] Once a device is contaminated it can be effectively cleaned by filling the micro- and nanochannels with a 10% sulfuric acid solution and allowing the device to sit overnight, followed by thoroughly rinsing the channels with water. We have used these devices for over 1 year with no observable change in performance.

In addition to the fabrication of nanochannels in quartz, this method is readily transferrable to other substrate materials, both hard and soft. Nanochannels were milled in Si(100) substrates through a 150-nm thick Al film. Aluminum, with a sputtering yield of 0.30 $\mu m^3$/nC, is not as effective as a masking layer as chromium.[27] It was selected because it does not as readily form a silicide upon ion irradiation as Cr does and because the Al etching solution (PAN etch, 16:2:1:1 $H_3PO_4$:$H_2O$:$CH_3COOH$:$HNO_3$) is compatible with Si.[31] Figure 6 shows SEM images of nanochannel cross-sections immediately after milling (Fig. 6a,c) and after Al removal (Fig. 6b,d). Although a metal film is not required to dissipate charge with semiconducting Si, the use of one yields nanochannels with a more uniform shape and smaller ultimate dimensions than can be achieved by milling directly into a Si substrate. This is made evident by comparing Figure 6e-f showing nanochannels milled directly into Si with those images of nanochannels milled through the Al film (Fig. 6b,d). The nanochannels shown in Fig. 6b and Fig. 6e and those shown in Fig. 6d and Fig. 6f were milled with similar ion beam parameters, respectively. Furthermore, the surface adjacent to a feature milled directly into a Si substrate is significantly deformed while the surface near a feature milled through an Al film has been protected. Figure 7 shows representative atomic force microscopy (AFM) profiles of 2-μm wide features milled into a Si substrate (MFP-3D atomic force microscope, Asylum Research). The regions are milled into a Si substrate directly (Fig. 7a) or through a 150-nm thick Al film (Fig. 7b). In Figure 7c these data are reduced to line profiles by averaging along the 1-μm length of the three-dimensional profiles (ca. 170 individual lines per profile). The protuberance observed along the edges of the feature milled directly into the Si substrate averages about 15 nm in height, consistent with observations in previous studies.[26,32] In contrast, the Al film appears to be effective in protecting the top Si surface from redeposition and irradiation-induced swelling. The edges of the feature milled through the Al film are slightly raised (~ 4 nm). We note that some lateral scattering of $Ga^+$ ions into the material occurs and the presence of the Al film would be ineffective in preventing material damage resulting from such collisions.

Finally, we investigated the use of this methodology for the patterning of soft materials, in this case polydimethylsiloxane (PDMS, Sylgard® 184, Dow Corning Corporation). In an attempt to leverage PDMS's elastomeric properties, a 130-nm thick Cr film was deposited and FIB milling performed on a piece of 1-mm thick PDMS that was stretched ~20% on a custom built specimen mount. The nanochannels were oriented such that the channel length and width were perpendicular and parallel to the stretch direction, respectively. After milling and while the sample was still stretched, the Cr film was removed and a thin (4 nm) Cr film was deposited to dissipate charge during SEM imaging. An SEM image of the nanochannel in the stretched PDMS substrate, having a width of 95 nm, is shown in Figure 8a. The 4-nm Cr film is then removed, the sample is relaxed, a new 4-nm Cr film is deposited and the sample is re-imaged (Fig. 8b). The nanochannel width is now 82 nm, a 14% decrease commensurate with the 17% decrease in the bulk dimensions of the PDMS upon relaxation. This demonstrates the broad applicability of our FIB milling strategy to a wide range of substrate materials and suggests a method for extending the ultimate dimensions accessible using FIB patterning by taking advantage of the materials properties of substrates and masking layers.

In conclusion, a general strategy for fabricating nanochannels with critical dimensions below 5 nm is presented. This method consists of FIB milling channels through a relatively

thick metal film into the underlying substrate. The use of a sufficiently thick metal film offers the advantages of smaller nanochannel dimensions and smoother surfaces along the nanochannel edges. These nanochannels can be incorporated into fluidic devices by interfacing them to microfluidic channels and by sealing the top surface of the channels with a cover plate. This methodology can be applied to both hard and soft materials of potential utility in nanofluidic technologies.

## Acknowledgments

This work was sponsored in part by a grant from the National Human Genome Research Institute, National Institutes of Health (R01HG02647-05). We thank J.P. Alarie and Valeri Gorbounov for valuable discussions. We also thank the staff of the Chapel Hill Analytical and Nanofabrication Laboratory (CHANL) for their support.

## References

1. Yuan Z, Garcia AL, Lopez GP, Petsev DN. Electrophoresis. 2007; 28:595. [PubMed: 17304495]
2. Schoch RB, Han J, Renaud P. Rev Mod Phys. 2008; 80:839.
3. Kovarik ML, Jacobson SC. Anal Chem. 2009; 81:7133. [PubMed: 19663470]
4. Lerman LS, Frisch HL. Biopolymers. 1982; 21:995. [PubMed: 7082773]
5. Tong HD, Jansen HV, Gadgil VJ, Bostan CG, Berenschot E, van Rijn CJM, Elwenspoek M. Nano Lett. 2004; 4:283.
6. Volkmuth WD, Austin RH. Nature. 1992; 358:600. [PubMed: 1501715]
7. Striemer CC, Gaborski TR, McGrath JL, Fauchet PM. Nature. 2007; 445:749. [PubMed: 17301789]
8. Reisner W, Morton KJ, Riehn R, Wang YM, Yu Z, Rosen M, Sturm JC, Chou SY, Frey E, Austin RH. Phys Rev Lett. 2005; 94:196101. [PubMed: 16090189]
9. Salieb-Beugelaar GB, Dorfman KD, van den Berg A, Eijkel JCT. Lab Chip. 2009; 9:2508. [PubMed: 19680576]
10. Douville N, Huh D, Takayama S. Anal Bioanal Chem. 2008; 391:2395. [PubMed: 18340435]
11. Mijatovic D, Eijkel JCT, van den Berg A. Lab Chip. 2005; 5:492. [PubMed: 15856084]
12. Perry JL, Kandlikar SG. Microfluid Nanofluid. 2006; 2:185.
13. Abgrall P, Nguyen NT. Anal Chem. 2008; 80:2326. [PubMed: 18321133]
14. Cross JD, Strychalski EA, Craighead HG. J Appl Phys. 2007; 102:024701.
15. Balducci A, Mao P, Han JY, Doyle PS. Macromolecules. 2006; 39:6273.
16. Salieb-Beugelaar GB, Teapal J, van Nieuwkasteele J, Wijnperlé D, Tegenfeldt JO, Lisdat F, van den Berg A, Eijkel JCT. Nano Lett. 2008; 8:1785. [PubMed: 18393468]
17. Cao H, Yu Z, Wang J, Tegenfeldt JO, Austin RH, Chen E, Wu W, Chou SY. Appl Phys Lett. 2002; 81:174.
18. Reisner W, Beech JP, Larsen NB, Flyvbjerg H, Kristensen A, Tegenfeldt JO. Phys Rev Lett. 2007; 99:058302. [PubMed: 17930801]
19. Campbell LC, Wilkinson MJ, Manz A, Camilleri P, Humphreys CJ. Lab Chip. 2004; 4:225. [PubMed: 15159783]
20. Riehn R, Lu M, Wang YM, Lim SF, Cox EC, Austin RH. Proc Natl Acad Sci USA. 2005; 102:10012. [PubMed: 16000405]
21. Fan R, Karnik R, Yue M, Li DY, Majumdar A, Yang PD. Nano Lett. 2005; 5:1633. [PubMed: 16159197]
22. Huh D, Mills KL, Zhu X, Burns MA, Thouless MD, Takayama S. Nat Mater. 2007; 6:424. [PubMed: 17486084]
23. Nikoobakht B. Chem Mater. 2009; 21:27.
24. Tseng AA. J Micromech Microeng. 2004; 14:R15.
25. Han J, Lee H, Min BK, Lee SJ. Microelectron Eng. 2010; 87:1.
26. Lugstein A, Basnar B, Smoliner J, Bertagnolli E. Appl Phys A. 2003; 76:545.
27. Orloff J, Swanson LW, Utlaut M. J Vac Sci Technol B. 1996; 14:3759.

28. Holzer L, Indutnyi F, Gasser PH, Münch B, Wegmann M. J Microsc. 2004; 216:84. [PubMed: 15369488]
29. Strychalski EA, Levy SL, Craighead HG. Macromolecules. 2008; 41:7716.
30. Haneveld J, Jansen H, Berenschot E, Tas N, Elwenspoek M. J Micromech Microeng. 2003; 13:S62.
31. Nakayama T, Sotome S, Shinji S. Microelectron Eng. 86:1718.
32. Li HW, Kang DJ, Blamire MG, Huck WTS. Nanotechnology. 2003; 14:220.

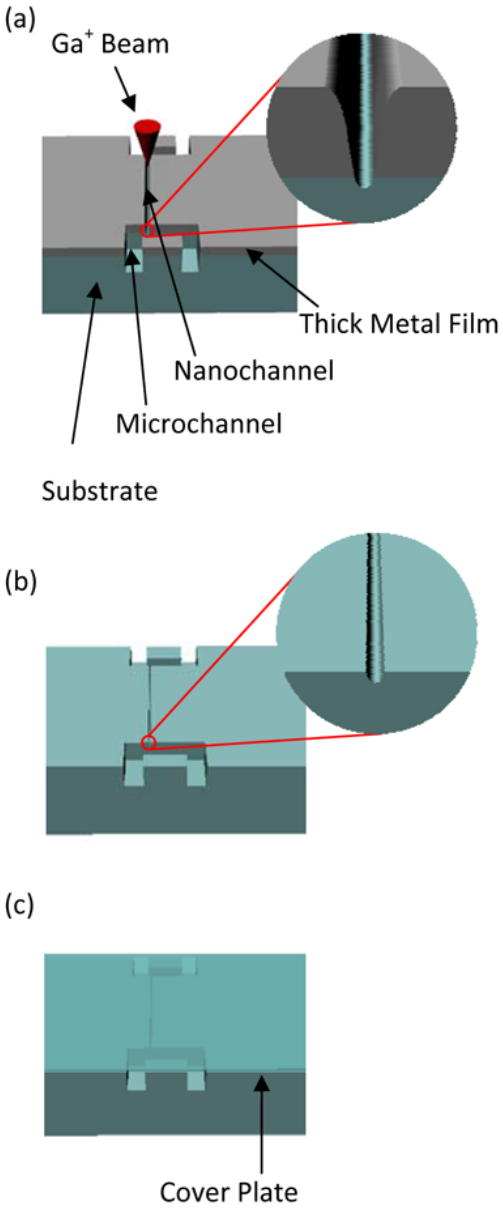


**Figure 1.**
Schematic drawing of the FIB milling process and subsequent fabrication steps. (a) Milling a nanochannel through the thick metal film. (b) Removal of the metal film using an etching solution. (c) Sealing of the micro- and nanochannels with a cover plate.

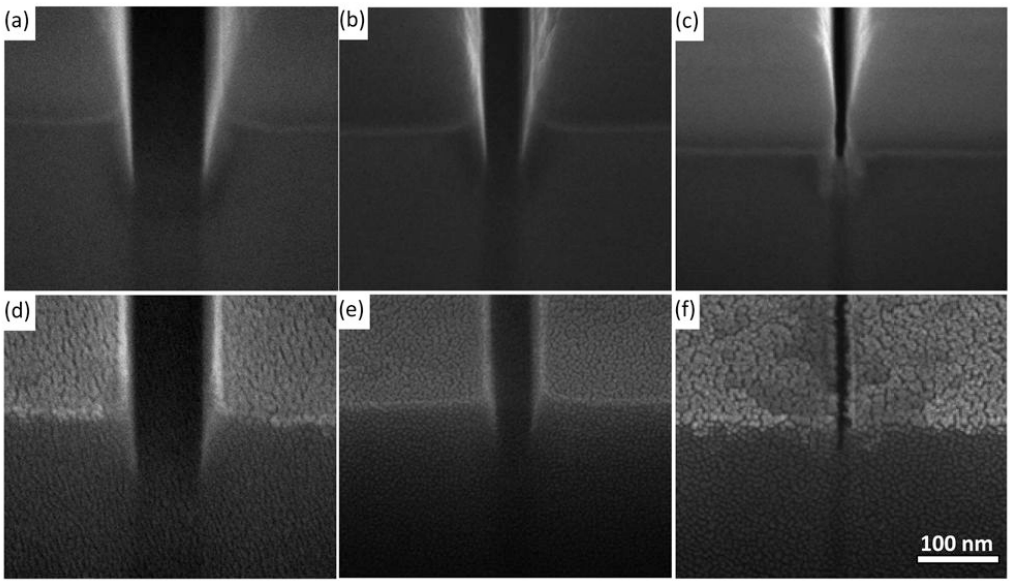


**Figure 2.**
SEM images of nanochannel cross-sections milled through a 130-nm Cr masking layer into a quartz substrate (a-c) before and (d-f) after Cr removal. (a,d) 100 nm × 100 nm; (b,e) 50 nm × 50 nm; (c,f) 12 nm × 12 nm. The roughness apparent in (d-f) is due to a 2-nm AuPd layer that is deposited for SEM imaging. Specimens are tilted 52° with respect to the electron beam.

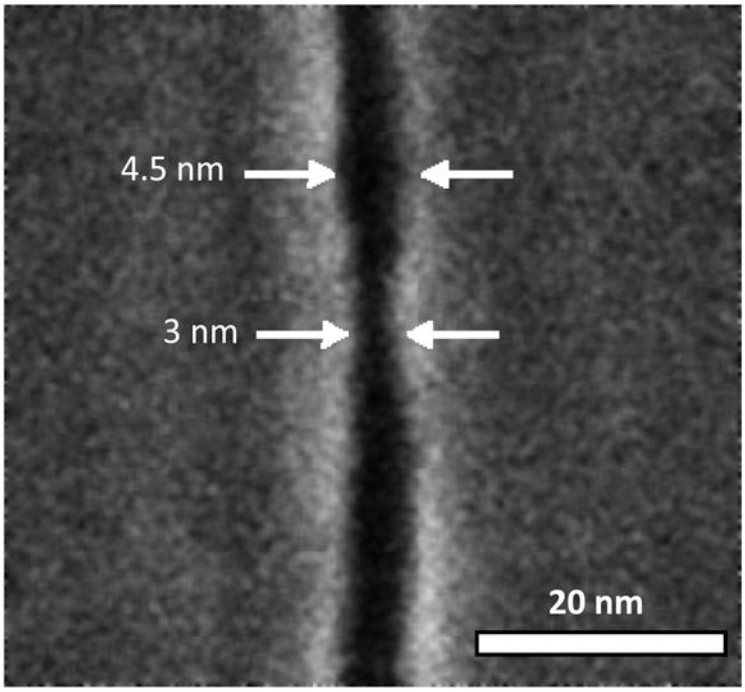


**Figure 3.**
Top-view SEM image of a sub-5-nm wide nanochannel milled into a quartz substrate through a 300-nm Cr layer.

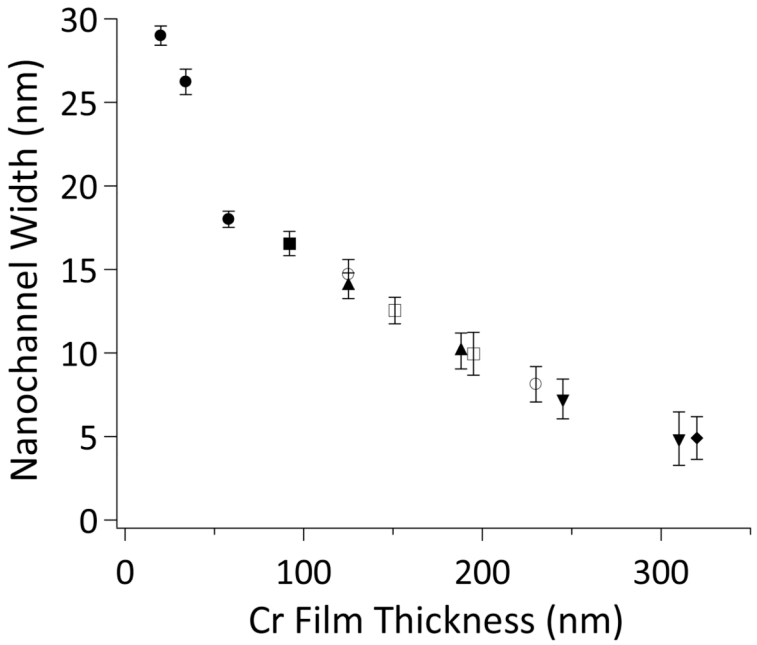


**Figure 4.**
Effect of the Cr film thickness on the width of nanochannels FIB milled into a quartz substrate using a 1.5-pA ion beam current. Different markers represent samples that were milled during 7 different sessions on the instrument. Each value was determined from width measurements made at multiple locations along at least three different channels (N=20 for each point).

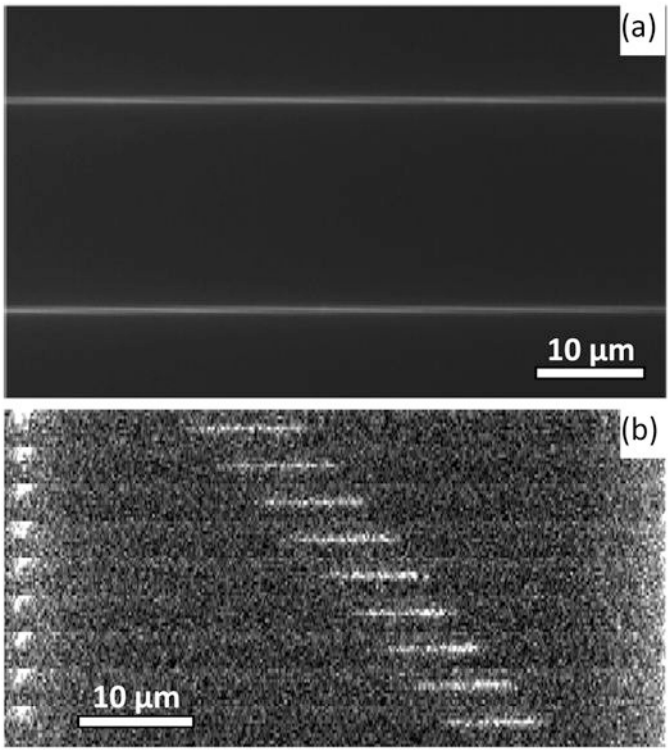


**Figure 5.**
(a) Fluorescence micrograph of 30-nm nanochannels filled with 2 mM fluorescein dye. (b) Series of frames recorded during the translocation of a single molecule of fluorescently-stained λ-phage DNA through a 50-nm channel. A frame is collected every 3 ms.

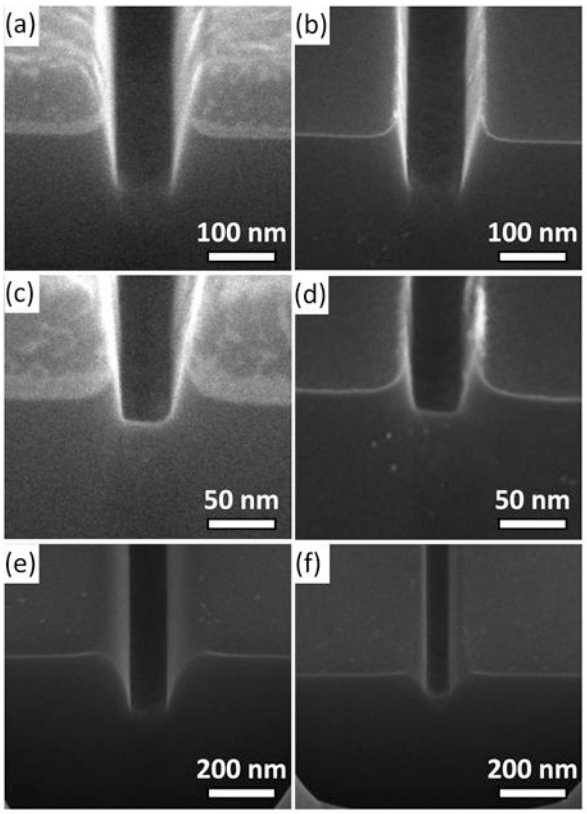


**Figure 6.**
Nanochannels milled in Si substrates. Channels milled in Si through a 150-nm Al layer before (a,c) and after (b,d) Al removal. The channel in (a,b) is ~100 nm in width and depth while that in (c,d) is ~35 nm in width and depth. (e) Channel milled directly into Si, 100 nm wide at bottom and 200 nm deep. (f) Channel milled directly in Si, 65 nm wide at bottom and 70 nm deep. Specimens are tilted 52° with respect to the electron beam.

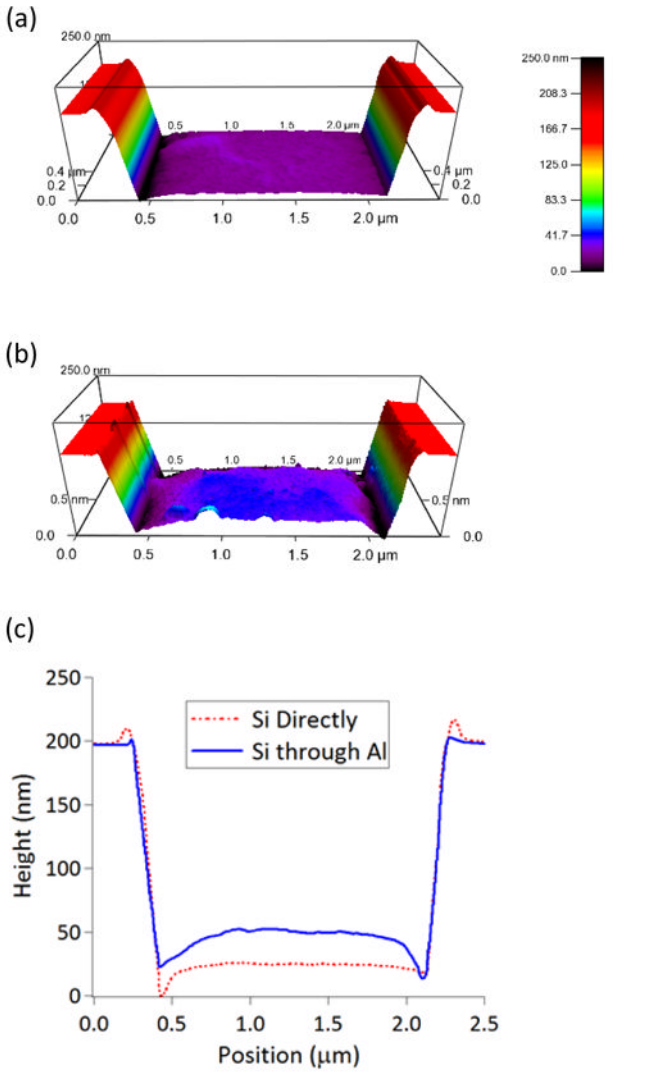


**Figure 7.**

(a) AFM profile of a 2-µm wide feature milled directly into a Si substrate. (b) AFM profile of a comparable feature milled into a Si substrate through a 150-nm thick Al film, followed by removal of the Al film by wet chemical etching. (c) Line profiles of the two samples obtained by averaging lines along the three-dimensional profiles in (a) and (b).

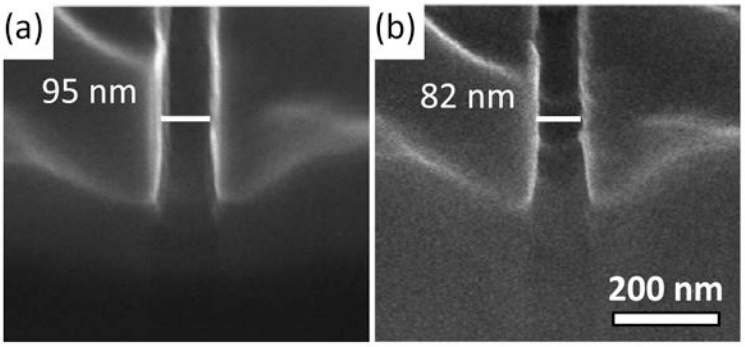


**Figure 8.**
SEM images of a nanochannel milled into a stretched PDMS substrate through a Cr masking layer. The 130-nm thick Cr film has been removed prior to imaging. (a) The nanochannel in the stretched PDMS and (b) after relaxation of the PDMS. Specimens are tilted 52° with respect to the electron beam.